Original article

MRI visibility of gold fiducial markers for image-guided radiotherapy of rectal cancer

Roy P.J. van den Ende [a,*], Lisanne S. Rigter [b], Ellen M. Kerkhof [a], Els L. van Persijn van Meerten [c], Eva C. Rijkmans [a], Doenja M.J. Lambregts [d], Baukelien van Triest [e], Monique E. van Leerdam [b], Marius Staring [a,f], Corrie A.M. Marijnen [a], Uulke A. van der Heide [a,e]

[a] Department of Radiation Oncology, Leiden University Medical Center; [b] Department of Gastroenterology, The Netherlands Cancer Institute, Amsterdam; [c] Department of Radiology, Leiden University Medical Center; [d] Department of Radiology, The Netherlands Cancer Institute, Amsterdam; [e] Department of Radiation Oncology, The Netherlands Cancer Institute, Amsterdam; and [f] Division of Image Processing, Department of Radiology, Leiden University Medical Center, Leiden, the Netherlands

ARTICLE INFO

ABSTRACT

Background and purpose: A GTV boost is suggested to result in higher complete response rates in rectal cancer patients, which is attractive for organ preservation. Fiducials may offer GTV position verification on (CB)CT, if the fiducial-GTV spatial relationship can be accurately defined on MRI. The study aim was to evaluate the MRI visibility of fiducials inserted in the rectum.

Materials and methods: We tested four fiducial types (two Visicoil types, Cook and Gold Anchor), inserted in five patients each. Four observers identified fiducial locations on two MRI exams per patient in two scenarios: without (scenario A) and with (scenario B) (CB)CT available. A fiducial was defined to be consistently identified if 3 out of 4 observers labeled that fiducial at the same position on MRI. Fiducial visibility was scored on an axial and sagittal T2-TSE sequence and a T1 3D GRE sequence.

Results: Fiducial identification was poor in scenario A for all fiducial types. The Visicoil 0.75 and Gold Anchor were the most consistently identified fiducials in scenario B with 7 out of 9 and 8 out of 11 consistently identified fiducials in the first MRI exam and 2 out of 7 and 5 out of 10 in the second MRI exam, respectively. The consistently identified Visicoil 0.75 and Gold Anchor fiducials were best visible on the T1 3D GRE sequence.

Conclusion: The Visicoil 0.75 and Gold Anchor fiducials were the most visible fiducials on MRI as they were most consistently identified. The use of a registered (CB)CT and a T1 3D GRE MRI sequence is recommended.

© 2018 The Author(s). Published by Elsevier B.V. Radiotherapy and Oncology xxx (2018) xxx–xxx This is an open access article under the CC BY-NC-ND license (http://creativecommons.org/licenses/by-nc-nd/4.0/).

Neoadjuvant radiotherapy plays an important role in the treatment of patients with rectal cancer since it reduces the rate of local recurrence [1–4]. After standard neoadjuvant chemoradiation, pathological complete response is observed in approximately 15–25% of patients [5,6]. In selected centers with a watch and wait approach, clinical complete response is observed in up to 50% of patients, probably due to better patient selection [7,8]. Dose response analyses suggest that higher tumor doses result in higher complete response rates in rectal cancer patients, which is attractive in the light of increased interest for organ preservation [6,9–11].

Tumor dose can be increased by applying a boost with external beam radiotherapy (EBRT), high-dose rate endorectal brachytherapy (HDREBT) or contact therapy. Current clinical practice for posi-

tion verification is megavolt imaging or cone beam computed tomography (CBCT) during EBRT and a radiograph or CT during HDREBT [12–15]. However, these imaging modalities suffer from limited soft tissue contrast which makes position verification of the gross tumor volume (GTV) difficult [16,17]. For HDREBT position verification, endoluminal clips have been used to indicate the proximal and distal borders of the tumor [18]. However, these clips create large artifacts on magnetic resonance imaging (MRI), which makes it impossible to determine the spatial relationship with the GTV accurately using MRI [19]. With the introduction of MR-guided radiotherapy systems, position verification of the GTV could be performed online with the superior soft-tissue contrast of MRI [20]. However, as MR-guided linear accelerators and in room MRI-HDR suites are not widely available, MRI compatible gold fiducials in combination with (CB)CT may offer an alternative for position verification of the GTV. The use of fiducials has been described for other tumor locations such as pancreas, esophagus

* Corresponding author: Department of Radiation Oncology, Leiden University Medical Center, P.O. Box 9600, 2300 RC Leiden, the Netherlands.

E-mail address: r.p.j.van_den_ende@lumc.nl (R.P.J. van den Ende).

and prostate and has been proven useful for position verification of the target volume during EBRT [21–23].

To determine the location of the GTV accurately on (CB)CT, the spatial relationship between the GTV and the fiducials should be determined on MRI and therefore the fiducials have to be visible on MRI. Several studies report good MRI visibility of fiducials in phantoms or other organs [24–26]. However, the presence of air and feces in the rectum may hamper fiducial visibility. Excellent fiducial visibility in the rectum has been reported on CT, but no analysis of MRI visibility has been performed to date [27,28]. The aim of this study was to evaluate the MRI visibility of different fiducials inserted in the tumor or mesorectum.

Materials and methods

Patient selection

Between July 2015 and September 2016, we included 20 patients at the Netherlands Cancer Institute (NKI) and at the Leiden University Medical Center (LUMC) with proven rectal adenocarcinoma who were scheduled for short-course radiotherapy (SC-RT; 5×5 Gy) or long course chemoradiotherapy (LC-CRT; 25×2 Gy combined with capecitabine 825 mg/m^2 twice daily) followed by a total mesorectal excision. Eleven patients received SC-RT and nine patients LC-CRT. Exclusion criteria were contraindication for fiducial insertion (coagulopathy or anticoagulants that cannot be stopped), prior pelvic irradiation, pelvic surgery or hip replacement surgery, pregnancy, world health organization performance status 3–4 and a contraindication for MRI. This study was registered at the Dutch Trial Registry (REMARK study, registration no. NTR4606) [29].

Fiducials

We tested four types of fiducials, inserted in five patients each (Visicoil 0.5 mm × 5 mm and Visicoil 0.75 mm × 5 mm [IBA Dosimetry, GmbH, Germany], Cook 0.64 mm × 3.4 mm [COOK Medical, Limerick, Ireland] and Gold Anchor 0.28 mm × 20 mm (unfolded length) [Naslund Medical AB, Sweden]. The Visicoil and Cook fiducials were straight, only differing in diameter and length. The Gold Anchor fiducial was also straight but could be folded when inserted, depending on the insertion technique. We have inserted the Gold Anchor fiducial in a folded configuration as it improves MRI visibility [24].

Four experienced gastroenterologists (two in each center) inserted 64 fiducials in 20 patients in the tumor or mesorectum at least one day before the start of radiotherapy by sigmoidoscopy or endoscopic ultrasonography. The target lesion was visualized and the absence of intervening vascular structures was verified before inserting each fiducial. In the first 10 patients, we aimed to insert three fiducials in the tumor tissue. Due to limited fiducial retention in these patients, in the last 10 patients we aimed to insert at least two fiducials in the mesorectal fat (one proximal and one distal of the tumor) and one in the center of the tumor.

Imaging

We acquired a planning CT scan before the start of radiotherapy on a Siemens Sensation Open (slice thickness 3.0–5.0 mm, pixel spacing 0.98–1.27 mm × 0.98–1.27 mm, 120 kVp, tube current 74–307 mA (automatic exposure control), exposure time 1100 ms, convolution kernel B40s) or a Philips Brilliance Big Bore (slice thickness 3.0 mm, pixel spacing 0.98–1.14 mm × 0.98–1.14 mm, 120 kVp, tube current 271 mA, exposure time 923 ms, convolution kernel B (Philips)). To evaluate reproducibility of fiducial visibility on MRI, we performed a pre-treatment MRI exam before the start of radiotherapy (from now on called first MRI) and a second MRI exam after completion of a week of radiotherapy (from now on called second MRI). MRI exams were performed in supine position on a standard MR table. Due to logistical reasons, for one patient a second MRI was not performed. MRI exams were performed on a Philips Achieva 1.5T, Philips Achieva 3T, Philips Achieva dStream 3T or a Philips Ingenia 3T. Two MRI exams were performed on the 1.5T MRI scanner, all other MRI exams were performed on 3T MRI scanners. We selected three MRI sequences for the fiducial visibility scoring, including a transverse 2D T2 turbo spin echo sequence (tT2-TSE), a sagittal 2D T2-TSE sequence (sT2-TSE) and a T1 3D gradient echo sequence (T1 3D GRE). The T1 3D GRE sequence was acquired with fat suppression in 16/20 scans in the first MRI and 14/19 scans in the second MRI. Scan parameters for the different MRI sequences are reported in Table I in the Supplementary Materials.

During the first week of radiotherapy, we acquired daily pre- and post-irradiation CBCT scans (reconstructed slice thickness 1.0 mm, pixel spacing 1.0 mm × 1.0 mm, 120 kVp, tube current 32 mA, exposure time 40 ms). Before the planning CT and each radiotherapy fraction, patients were asked to void their bladder and subsequently drink 300 cc of water to reproduce bladder filling.

As all fiducials were well visible on (CB)CT, we registered and subsequently resampled a (CB)CT scan to the T1 3D GRE sequence of each MRI exam with a rigid registration with a mutual information metric using Elastix [30]. The registration was assessed by a single observer (RE) by checking the alignment of the bony anatomy. We used the (CB)CT scan that was acquired closest to the acquisition date of the MRI exam. The T1 3D GRE sequence was chosen for the registration as it had the highest resolution. As all MRI sequences were acquired within the same MRI exam without table movement between sequences, no registration was performed between the sequences.

Images were visualized with an in-house developed user interface, created in MeVisLab 2.7.1 (MeVis Medical Solutions AG, Fraunhofer MEVIS, Bremen, Germany). The user interface automatically determines a window/level setting depending on the image set that is shown. The automatically determined window was defined as the difference between the minimum and maximum image pixel value and the level was defined as the mean of the minimum and maximum image pixel value. All observers were therefore presented with images with initially the same window/level settings when performing the fiducial visibility scoring. In addition, observers were able to manually change the window/level settings.

Fiducial visibility scoring

Fiducial visibility was scored by two radiologists with expertise in rectal imaging (EP and DL), a radiation-oncologist (BT) and a resident radiation-oncologist (ER). Observers were blinded for fiducial type and each other's results.

Fiducial visibility was scored according to two scenarios. In scenario A, only the MRI images and clinical information (endoscopic findings and number and location of inserted fiducials) were available to the observers. In scenario B, the MRI images, clinical information as well as the rigidly registered CB(CT) scan were at the observer's disposal. For the first MRI, visibility scoring according to scenarios A and B was subsequently performed within one scoring session; for the second MRI, only scenario B was performed.

For each scenario, the observers first scored the fiducials on the first MRI for each patient and at a later stage on the second MRI for each patient. For both MRI exams the observers analyzed patients in random patient order. The observers rated the fiducial visibility on each available MRI sequence (not visible, poor/average or

good/excellent) and rated how confident they were that the identified fiducial position really represented a fiducial and not for example an air artifact (not very confident, moderately confident, or very confident). Observers were then instructed to identify and label fiducial positions on the MRI sequence on which they could identify the fiducial location most accurately. Identified fiducial positions were saved in world coordinates.

We used the (CB)CT as a reference to determine the number of fiducials present in a patient at the time of the MRI exam. In combination with the soft tissue information from the MRI scan, we determined whether the fiducial was inserted in the tumor or the mesorectum. (CB)CT was not used as a reference to determine the position of the fiducials on MRI because of the limited soft tissue contrast which made deformable registration with MRI not feasible. Instead, the standard of reference for fiducial location on MRI was defined as the consistent identification of a fiducial on the same position on MRI by at least three out of four observers. This was determined by calculating the distances between the identifications of all observers using the world coordinates of the identifications. Identification pairs with a distance of less than 5 mm between observers were subsequently analyzed visually to check whether the same artifact was labeled.

Statistical analysis

We used SPSS Statistics 23 (IBM Corp. Released 2015. IBM SPSS Statistics for Windows, Version 23.0. Armonk, NY: IBM Corp.) for statistical analysis. The Wilcoxon signed rank test was used to test for differences in visibility rating between MRI sequences. All tests were two-sided and the significance threshold was set at 0.05.

Results

A total of 64 fiducials was inserted in 20 patients. A planning CT with fiducials was available in 10/20 patients. In the other 10 patients, fiducials were inserted after the planning CT. Median time between fiducial insertion and the first MRI exam was 3 days (range 0–11 days), between any MRI exam and the corresponding reference scan 0 days (range 0–5 days) and between the first and second MRI exam 7 days (range 4–21). At the time of the first MRI, 39 fiducials were still in situ in the tumor or mesorectum, based on evaluation on (CB)CT. At the time of the second MRI, 35 fiducials were still in situ. The remaining 29 fiducials were either lost between insertion and the first MRI ($n = 18$), lost between the two MRI exams ($n = 4$), inadvertently inserted in the prostate ($n = 5$), or simultaneously ejected during insertion and therefore so close together that they were analyzed as one fiducial ($n = 2$). For the nine patients that received LC-CRT, the CBCT scans that were acquired after the first week of radiotherapy showed that no further fiducials were lost during the course of treatment. Nine fiducials were inserted in the mesorectum (one Visicoil 0.5, two Visicoil 0.75, three Cook and three Gold Anchor fiducials) and thirty fiducials were inserted in the tumor (eight Visicoil 0.5, seven Visicoil 0.75, six COOKs and nine Gold Anchors). In five out of nine mesorectum fiducials in four patients a T1 3D GRE sequence was performed with fat suppression and therefore these fiducials were excluded from further analyses (one Visicoil 0.5, three COOKs and one Gold Anchor). None of these fiducials were consistently identified. An overview of patient characteristics, type of reference scan and number of fiducials on reference scan is provided for each patient in Table 1. All registrations of (CB)CT scans to corresponding MRI exams were assessed by a single observer (RE) and considered to be sufficiently aligned for the purpose of this study: giving an approximate location of the fiducial on MRI.

Table 2 shows an overview of the consistent and inconsistent fiducial identifications with corresponding confidence levels. In scenario A of the first MRI, 2/9 Visicoil 0.75, 1/6 Cook and 5/11 Gold Anchor fiducials were consistently identified with an average distance between identifications of 1.8 mm (range 0.0–3.8 mm). Of those, two Visicoil 0.75, one Cook and four Gold Anchor fiducials were subsequently also consistently identified in scenario B. In scenario B of the first MRI, a total of 17 fiducials were consistently identified with an average distance between identifications of 2.0 mm (range 0.0–5.1 mm). Because of the low number of consistently identified fiducials in scenario A compared to scenario B, scenario A was not performed for the second MRI. For the second MRI, nine fiducials were consistently identified with an average distance between identifications of 0.9 mm (range 0.0–1.9 mm). In scenario B, the Visicoil 0.75 and the Gold Anchor fiducials were the most consistently identified fiducial types with 7/9 fiducials in 4 patients and 8/11 fiducials in 5 patients in the first MRI and 2/7 fiducials in 2 patients and 5/10 fiducials in 4 patients in the second MRI, respectively. Examples of fiducials on (CB)CT and corresponding MRI sequences are shown in Fig. 1. The fiducials shown in Fig. 1 were consistently identified. Table 3 shows the difference between observers for the Visicoil 0.75 and Gold Anchor fiducial identifications. Observer 4 had a substantially lower number of consistently identified fiducials and labeled more fiducials on MRI than the number of fiducials present on the reference scan. For observer 3 and 4 in the second MRI of the Visicoil 0.75, one confidence level was missing.

The visibility rating for the consistently identified Visicoil 0.75 and Gold Anchor fiducials per MRI sequence for both MRI exams is shown in Table 4. For the Visicoil 0.75, in the first MRI the tT2-TSE scored better visibility compared to the sT2-TSE sequence ($p = 0.03$). The T1 3D GRE sequence scored better visibility compared to the tT2-TSE ($p = 0.03$) and the sT2-TSE ($p = 0.01$). In the second MRI, T1 3D GRE scored better visibility compared to the sT2-TSE ($p = 0.04$). For the Gold Anchor, in the first MRI the T1 3D GRE scored better visibility compared to the sT2-TSE ($p = 0.02$). No other statistically significant differences were observed. In addition, Table 4 shows on which MRI sequence the fiducial positions were labeled, which is the sequence on which the fiducial could most accurately be identified according to the observers. For both the Visicoil 0.75 and the Gold Anchor fiducials, the T1 3D GRE sequence was chosen most often in both MRI exams.

Discussion

The aim of this study was to evaluate the MRI visibility of different fiducials inserted in the tumor or mesorectum. The results show that there are substantial differences in the number of consistently identified fiducials between fiducial types. For both the Visicoil 0.5 and the COOK fiducials, only one fiducial was consistently identified in both MRI exams (Table 2). These fiducial types were the smallest included in this study, which may explain the poor MRI visibility. This result confirms that of a study by Chan et al. who described the visibility of different types of fiducials in a phantom on CBCT, CT, megavolt imaging and MRI [26]. The authors concluded that fiducials with a diameter of 0.5 mm are poorly visible on MRI, even in a phantom. The Visicoil 0.75 has a larger diameter compared to the Visicoil 0.5 and the Cook fiducial, which may explain the better performance of this fiducial. The performance of the Gold Anchor fiducial is in line with a study by Gurney-Champion et al., who evaluated and characterized the visibility of different fiducials in a phantom on CT and MRI and included an in-vivo analysis of four patients in whom fiducials were inserted in the pancreas [24]. The authors recommend a Gold

Table 1
Patient characteristics, type of reference scan and number of fiducials on reference scan.

Patient	Sex	Age	cTNM	Tx	Fiducial type	Number of inserted fiducials	First MRI Reference scan	Number of fiducials on reference scan[*]	Second MRI Reference scan	Number of fiducials on reference scan[*]
1	M	71	T3N0M0	SC-RT	Visicoil 0.5	3	CT	2	CBCT	1
2	M	82	T3N0M0	SC-RT	Visicoil 0.5	3	CBCT	2	CBCT	2
3	M	63	T2N0M0	LC-CRT	Visicoil 0.5	3	CBCT	0	CBCT	0
4	M	60	T3N1M0	LC-CRT	Visicoil 0.5	3	CBCT	3	CBCT	3
5	F	60	T3N1M0	SC-RT	Visicoil 0.5	3	CBCT	1	CBCT	1
6	M	67	T3N2M0	LC-CRT	Visicoil 0.75	3	CT	3	CBCT	1
7	F	52	T3N1M0	SC-RT	Visicoil 0.75	3	CT	2	CBCT	2
8	M	75	T3N0M0	SC-RT	Visicoil 0.75	3	CBCT	2	CBCT	2
9	M	82	T2N1M0	SC-RT	Visicoil 0.75	3	CBCT	1	CBCT	1
10	M	63	T3N1M0	SC-RT	Visicoil 0.75	3	CBCT	1	CBCT	1
11	F	62	T2N1M0	SC-RT	COOK	3	CT	2	CBCT	2
12	M	58	T3N0M0	LC-CRT	COOK	4	CBCT	0	–	–
13	M	57	T3N2M0	LC-CRT	COOK	4	CBCT	1	CBCT	1
14	F	60	T3N1M0	SC-RT	COOK	4	CBCT	1	CBCT	1
15	M	59	T3N2M0	LC-CRT	COOK	4	CBCT	2	CBCT	2
16	M	63	T3N0M0	LC-CRT	Gold Anchor	3	CBCT	2	CBCT	2
17	M	65	T3N2M0	LC-CRT	Gold Anchor	3	CBCT	2	CBCT	1
18	M	59	T2N1M0	SC-RT	Gold Anchor	3	CBCT	2	CBCT	2
19	F	61	T3N1M0	SC-RT	Gold Anchor	3	CBCT	3	CBCT	3
20	M	51	T3N0M0	LC-CRT	Gold Anchor	3	CBCT	2	CBCT	2

M = male, F = female, Tx = treatment schedule, SC-RT = short course radiotherapy, LC-CRT = long course chemoradiotherapy.
[*] The number of fiducials on the reference scan excludes fiducials that were inadvertently inserted in the prostate and fiducials in the mesorectum in which the T1 3D GRE was performed with fat suppression.

Anchor fiducial in a folded configuration when MRI visibility is desired.

The fiducial insertion strategy was changed during the study because insertion of fiducials in the tumor resulted in a low fiducial retention rate. Since only nine out of 39 fiducials were inserted in the mesorectum and five of those were scanned with fat suppression on the T1 3D GRE sequence, no firm conclusions can be drawn on the difference in fiducial detection between fiducials in the tumor and the mesorectum.

Eight out of eleven Gold Anchor fiducials were consistently identified in the first MRI, while only five out of ten Gold Anchors fiducials were consistently identified in the second MRI (Table 2). One identified Gold Anchor fiducial was lost in between the MRI exams, as evaluated on CBCT. For the two Gold Anchor fiducials in two patients that were no longer identified in the second MRI,

the first and the second MRI were compared. Air or feces deformed the rectum which made correlation with the CBCT scan difficult. In addition, the artifacts caused by air further hampered fiducial detection. For the Visicoil 0.75, only two out of seven fiducials were consistently identified in the second MRI, compared to seven out of nine in the first MRI. Two consistently identified fiducials were lost in between the MRI exams. The remaining three fiducials were no longer consistently identified in the second MRI as they were identified by only two out of four observers.

Even with the two best visible fiducials in this study, it can be argued whether the obtained performance justifies the use of fiducials in the rectum in clinical practice. For instance, reproducibility of the observer identifications between the MRI exams was limited, as shown by the lower number of consistently identified fiducials in the second MRI for Visicoil 0.75 and Gold Anchor. In addition,

Table 2
Number of consistent and inconsistent identifications for all observers for scenario B with corresponding confidence levels, split according to fiducial type.

	Visicoil 0.5	Visicoil 0.75	COOK	Gold Anchor
First MRI Exam, scenario B				
Fiducials on corresponding (CB)CT	8	9	6	11
Total identifications by 4 observers[*]	22 (32)	34 (36)	26 (24)	43 (44)
Inconsistent identifications	19	13	22	14
Consistent identifications	3	21	4	29
Which represent number of consistently identified fiducials	1/8 (13%)	7/9 (78%)	1/6 (17%)	8/11 (73%)
Of which were already consistently identified in **scenario A**	0/8 (0%)	2/9 (22%)	1/6 (17%)	5/11 (45%)
Confidence level for all identifications				
Not very confident	9 (41%)	2 (6%)	12 (46%)	6 (14%)
Moderately confident	7 (32%)	10 (29%)	7 (27%)	7 (16%)
Very confident	6 (27%)	22 (65%)	7 (27%)	30 (70%)
Second MRI exam, scenario B				
Fiducials on corresponding (CB)CT	7	7	6	10
Total identifications by 4 observers[*]	22 (28)	25 (28)	20 (24)	40 (40)
Inconsistent identifications	18	19	17	23
Consistent identifications	4	6	3	17
Which represent number of consistently identified fiducials	1/7 (14%)	2/7 (29%)	1/6 (17%)	5/10 (50%)
Confidence level for all identifications				
Not very confident	4 (18%)	3 (13%)	9 (45%)	7 (18%)
Moderately confident	3 (14%)	9 (39%)	7 (35%)	21 (52%)
Very confident	15 (68%)	11 (48%)	4 (20%)	12 (30%)

[*] Numbers between brackets indicate the maximum number of correct identifications by four observers.
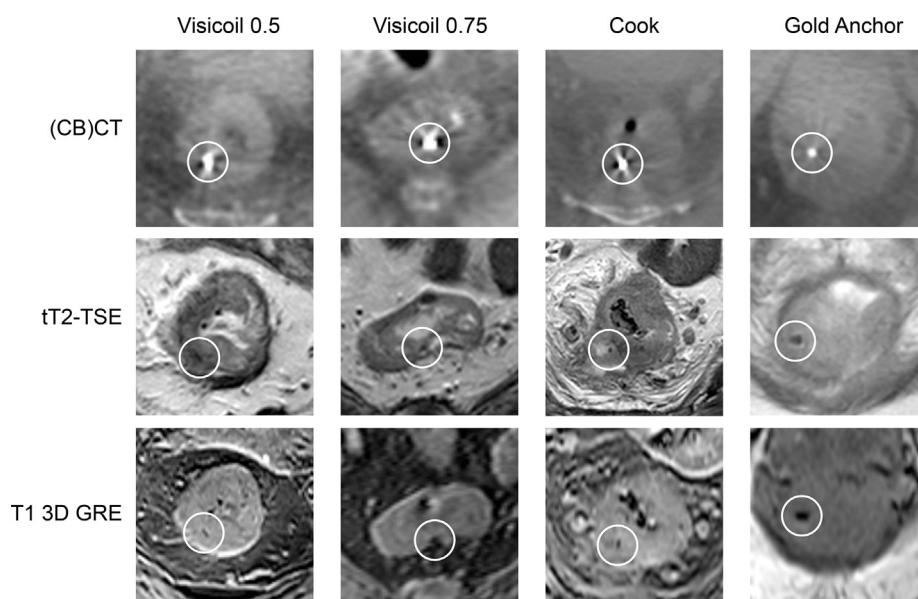
Fig. 1. Examples of fiducials shown on (CB)CT and corresponding MRI sequences.

Table 3
Number of consistently identified Visicoil 0.75 and Gold Anchor fiducials with corresponding confidence levels for each observer.

	Observer 1	Observer 2	Observer 3	Observer 4
Visicoil 0.75				
First MRI exam, scenario B				
Number of identifications	7/9	7/9	9/9	11/9
Of which are consistently labeled identifications	6	7	7	1
Confidence level for all identifications				
Not very confident	1 (14%)	0 (0%)	0 (0%)	1 (9%)
Moderately confident	2 (29%)	2 (29%)	3 (33%)	3 (27%)
Very confident	4 (57%)	5 (72%)	6 (67%)	7 (64%)
Second MRI exam, scenario B				
Number of identifications	5/7	4/7	7/7	9/7
Of which are consistently labeled identifications	2	2	2	0
Confidence level for all identifications				
Not very confident	1 (20%)	1 (25%)	0 (0%)	1 (13%)
Moderately confident	1 (20%)	3 (75%)	4 (67%)	1 (13%)
Very confident	3 (60%)	0 (0%)	2 (33%)	6 (75%)
Gold Anchor				
First MRI exam, scenario B				
Number of identifications	10/11	9/11	12/11	12/11
Of which are consistently labeled identifications	7	8	8	6
Confidence level for all identifications				
Not very confident	2 (20%)	1 (11%)	1 (8%)	2 (17%)
Moderately confident	2 (20%)	1 (11%)	2 (17%)	2 (17%)
Very confident	6 (60%)	7 (78%)	9 (75%)	8 (67%)
Second MRI exam, scenario B				
Number of identifications	8/10	8/10	11/10	13/10
Of which are consistently labeled identifications	5	5	5	2
Confidence level for all identifications				
Not very confident	3 (38%)	0 (0%)	0 (0%)	4 (31%)
Moderately confident	3 (38%)	5 (63%)	5 (46%)	8 (62%)
Very confident	2 (25%)	3 (38%)	6 (55%)	1 (8%)

inconsistencies between observers were observed, especially for the Visicoil 0.75 (Table 3). This suggests that it is worthwhile to have at least two observers to identify the fiducial positions on MRI. Furthermore, more fiducials may be inserted to increase the chance that sufficient fiducials will be identified for position verification (e.g. two or three).

The anatomical 2D T2-TSE sequences scored lower visibility with the Visicoil 0.75 fiducials compared to the Gold Anchor fiducials. This may be explained by the smaller size of the Visicoil 0.75 fiducials, which results in smaller signal voids on MRI. The signal voids may have been too small on the T2-TSE sequences. It is therefore not sufficient to use these MRI sequences alone to identify fiducial positions on MRI. The T1 3D GRE sequence scored higher fiducial visibility for both MRI exams for the Visicoil 0.75 and the first MRI exam for the Gold Anchor and was most often chosen to label the fiducial position on in all cases (Table 4). It is therefore recommended to include a T1 3D GRE sequence.

The T1 3D GRE sequence was a single-echo sequence acquired with a TE of about 2 ms. Two studies that evaluated fiducial visibility in the prostate reported promising results on the use of

Table 4
Visibility rating per MRI sequence for the consistently identified Visicoil 0.75 and Gold Anchor fiducials in scenario B of both MRI exams. In addition, the MRI sequence on which the fiducial positions were labeled is shown.

	tT2-TSE	sT2-TSE	T1 3D GRE
Visicoil 0.75			
First MRI exam, scenario B			
Not visible	1 (5%)	6 (29%)	0 (%)
Poor/average	12 (57%)	7 (33%)	9 (43%)
Good/excellent	8 (38%)	8 (38%)	12 (57%)
Labeled sequence	2/21 (10%)	2/21 (10%)	17/21 (81%)
Second MRI exam, scenario B			
Not visible	0 (0%)	4 (67%)	0 (0%)
Poor/average	4 (67%)	1 (17%)	2 (33%)
Good/excellent	2 (33%)	1 (17%)	4 (67%)
Labeled sequence	0/6 (0%)	1/6 (17%)	5/6 (83%)
Gold anchor			
First MRI Exam, scenario B			
Not visible	3 (10%)	4 (14%)	2 (7%)
Poor/average	9 (31%)	10 (35%)	5 (17%)
Good/excellent	17 (59%)	15 (52%)	22 (76%)
Labeled sequence	8/29 (28%)	4/29 (14%)	17/29 (59%)
Second MRI exam, scenario B			
Not visible	1 (6%)	3 (18%)	1 (6%)
Poor/average	5 (29%)	7 (41%)	6 (35%)
Good/excellent	11 (65%)	7 (41%)	10 (59%)
Labeled sequence	0/17 (0%)	7/17 (41%)	10/17 (59%)

a multi-echo gradient echo sequence [25,31]. The multi-echo gradient echo sequence results in multiple image sets with increasing TE which results in increased signal void size. It could be worthwhile to include this sequence in future studies, possibly enhancing fiducial identification.

Moningi et al. evaluated the role of fiducials in patients receiving neo-adjuvant endorectal brachytherapy in 11 rectal cancer patients [28]. The visibility of two types of fiducials was evaluated on CT by a radiologist, in which a subjective scoring system similar to this study was used. The radiologist scored all fiducials as clearly visible. The authors mention that both types of fiducials created a void on MRI that could assist with treatment planning, but no similar visibility analysis was performed to support this statement.

This study focused on gold fiducials, while other types of fiducials might be of interest. Liquid markers such as a hydrogel marker were not included because of poor stability, most likely because of absorption in the tissue [32]. Recent studies report on a liquid marker that forms a semisolid gel after injection [33,34]. Rydhog et al. reports on 15 lung cancer patients in whom markers were injected in the lymph nodes or the tumor. The authors found that the markers were well visible on CT and CBCT and stable in size and position throughout the treatment [33]. Schneider et al. evaluated gold fiducials and the liquid marker in a gel phantom that mimics the relaxation properties of pancreatic tissue. The authors show that the liquid markers cause signal voids on MRI due to the absence of water protons, equally affecting all MRI sequences [34]. This is contrary to gold fiducials, which also cause signal voids due to their effect on $T2^*$ of the surrounding tissue [24]. Therefore, the potential visibility of gold fiducials and the artifact size are correlated. As a result, better gold fiducial visibility because of increased TE also results in larger artifacts caused by air.

There are some limitations to this study. Only 39 fiducials were available for the visibility analysis because some fiducials were lost between insertion and the first MRI and five fiducials were inadvertently inserted in the prostate. Because of the low number of available fiducials per fiducial type, no statistical tests were performed to test for differences in consistent identifications between fiducial types.

The observers were blinded for fiducial type. As the artifact size differs substantially between fiducial types, results might have

been better if observers had known what artifact size to look for [24]. Since we defined a fiducial consistently identified if at least three out of four observers identified that fiducial position on the same position on MRI, inconsistently identified fiducials may still be true fiducials, but only identified by one or two observers.

There is no gold standard for the location of the fiducials on MRI. The rigid registration with (CB)CT provides an estimation of the location and may be inaccurate when day-to-day differences in rectal position and shape occur. Non-rigid registration was attempted for both the planning CT and CBCT scans, but was not considered feasible because of limited soft-tissue contrast, particularly on CBCT (35 out of 39 reference scans). Additionally, differences in rectal filling and differences in the presence and volume of air in the rectum further hampered non-rigid registration. Clinical practice does not include instructions on a diet or voiding of the rectum before the radiotherapy fraction. In addition, voiding of the bladder and drinking instructions were not applied before the MRI exam. If the drinking protocol would be applied to MRI and instructions on a diet or voiding of the rectum would be used, the correspondence between patient anatomy on CBCT and MRI may improve.

In conclusion, the Visicoil 0.75 and Gold Anchor fiducials were the best visible fiducials on MRI as it were the most consistently identified fiducials. Anatomical 2D T2-TSE MRI sequences are not sufficient to identify fiducials. Therefore, a T1 3D GRE sequence is recommended. The use of a corresponding (CB)CT scan improves fiducial detection on MRI. However, even for the best two fiducial types in this study, fiducial identification on MRI is challenging as shown by limited reproducibility between MRI exams and inconsistencies between observers. It is therefore recommended to have at least two observers and to further optimize MRI sequences to enhance the visibility of the fiducials.

Conflict of interest statement

Cook Medical fiducials were provided without costs. The producers of all fiducials had no involvement in the study design, in the collection, analysis and interpretation of data, in the writing of the manuscript and in the decision to submit the manuscript for publication.

Appendix A. Supplementary data

Supplementary data to this article can be found online at https://doi.org/10.1016/j.radonc.2018.11.016.

References

[1] Van Gijn W, Marijnen CAM, Nagtegaal ID, Kranenbarg EMK, Putter H, Wiggers T, et al. Preoperative radiotherapy combined with total mesorectal excision for resectable rectal cancer: 12-year follow-up of the multicentre, randomised controlled TME trial. Lancet Oncol 2011;12:575–82. https://doi.org/10.1016/S1470-2045(11)70097-3.

[2] Bosset JF, Calais G, Mineur L, Maingon P, Stojanovic-Rundic S, Bensadoun RJ, et al. Fluorouracil-based adjuvant chemotherapy after preoperative chemoradiotherapy in rectal cancer: Long-term results of the EORTC 22921

randomised study. Lancet Oncol 2014;15:184–90. https://doi.org/10.1016/S1470-2045(13)70599-0.

[3] Sauer R, Liersch T, Merkel S, Fietkau R, Hohenberger W, Hess C, et al. Preoperative versus postoperative chemoradiotherapy for locally advanced rectal cancer: Results of the German CAO/ARO/AIO-94 randomized phase III trial after a median follow-up of 11 years. J Clin Oncol 2012;30:1926–33. https://doi.org/10.1200/JCO.2011.40.1836.

[4] Sebag-Montefiore D, Stephens RJ, Steele R, Monson J, Grieve R, Khanna S, et al. Preoperative radiotherapy versus selective postoperative chemoradiotherapy in patients with rectal cancer (MRC CR07 and NCIC-CTG C016): a multicentre, randomised trial. Lancet 2009;373:811–20. https://doi.org/10.1016/S0140-6736(09)60484-0.

[5] Maas M, Nelemans PJ, Valentini V, Das P, Rödel C, Kuo LJ, et al. Long-term outcome in patients with a pathological complete response after chemoradiation for rectal cancer: A pooled analysis of individual patient data. Lancet Oncol 2010;11:835–44. https://doi.org/10.1016/S1470-2045(10)70172-8.

[6] Sanghera P, Wong DWY, McConkey CC, Geh JI, Hartley A. Chemoradiotherapy for rectal cancer: an updated analysis of factors affecting pathological response. Clin Oncol 2008;20:176–83. https://doi.org/10.1016/j.clon.2007.11.013.

[7] Maas M, Lambregts DMJ, Nelemans PJ, Heijnen LA, Martens MH, Leijtens JWA, et al. Assessment of clinical complete response after chemoradiation for rectal cancer with digital rectal examination, endoscopy, and MRI: selection for organ-saving treatment. Ann Surg Oncol 2015;22:3873–80. https://doi.org/10.1245/s10434-015-4687-9.

[8] Habr-Gama A, Gama-Rodrigues J, São Julião GP, Proscurshim I, Sabbagh C, Lynn PB, et al. Local recurrence after complete clinical response and watch and wait in rectal cancer after neoadjuvant chemoradiation: Impact of salvage therapy on local disease control. Int J Radiat Oncol Biol Phys 2014;88:822–8. https://doi.org/10.1016/j.ijrobp.2013.12.012.

[9] Appelt AL, Ploen J, Vogelius IR, Bentzen SM, Jakobsen A. Radiation dose-response model for locally advanced rectal cancer after preoperative chemoradiation therapy. Int J Radiat Oncol Biol Phys 2013;85:74–80. https://doi.org/10.1016/j.ijrobp.2012.05.017.

[10] Hall MD, Schultheiss TE, Smith DD, Fakih MG, Wong JYC, Chen YJ. Effect of increasing radiation dose on pathologic complete response in rectal cancer patients treated with neoadjuvant chemoradiation therapy. Acta Oncol (Madr) 2016;55:1392–9. https://doi.org/10.1080/0284186X.2016.1235797.

[11] Ortholan C, Romestaing P, Chapet O, Gerard JP. Correlation in rectal cancer between clinical tumor response after neoadjuvant radiotherapy and sphincter or organ preservation: 10-year results of the Lyon R 96–02 randomized trial. Int J Radiat Oncol Biol Phys 2012;83. https://doi.org/10.1016/j.ijrobp.2011.12.002.

[12] Vuong T, Devic S. High-dose-rate pre-operative endorectal brachytherapy for patients with rectal cancer. J Contemp Brachytherapy 2015;7:181–6. https://doi.org/10.5114/jcb.2015.51402.

[13] Nout RA, Devic S, Niazi T, Wyse J, Boutros M, Pelsser V, et al. CT-based adaptive high-dose-rate endorectal brachytherapy in the preoperative treatment of locally advanced rectal cancer: technical and practical aspects. Brachytherapy 2016;15:477–84. https://doi.org/10.1016/j.brachy.2016.03.004.

[14] Nijkamp J, de Jong R, Sonke JJ, Remeijer P, van Vliet C, Marijnen C. Target volume shape variation during hypo-fractionated preoperative irradiation of rectal cancer patients. Radiother Oncol 2009;92:202–9. https://doi.org/10.1016/j.radonc.2009.04.022.

[15] Tournel K, De Ridder M, Engels B, Bijdekerke P, Fierens Y, Duchateau M, et al. Assessment of intrafractional movement and internal motion in radiotherapy of rectal cancer using megavoltage computed tomography. Int J Radiat Oncol Biol Phys 2008;71:934–9. https://doi.org/10.1016/j.ijrobp.2008.02.032.

[16] O'Neill BDP, Salerno G, Thomas K, Tait DM, Brown G. MR vs CT imaging: Low rectal cancer tumour delineation for three-dimensional conformal radiotherapy. Br J Radiol 2009;82:509–13. https://doi.org/10.1259/bjr/60198873.

[17] Khoo VS, Joon DL. New developments in MRI for target volume delineation in radiotherapy. Br J Radiol 2006;79. https://doi.org/10.1259/bjr/41321492.

[18] Vuong T, Devic S, Moftah B, Evans M, Podgorsak EB. High-dose-rate endorectal brachytherapy in the treatment of locally advanced rectal carcinoma: technical aspects. Brachytherapy 2005;4:230–5. https://doi.org/10.1016/j.brachy.2005.03.006.

[19] Swellengrebel HAM. Evaluating long-term attachment of two different endoclips in the human gastrointestinal tract. World J Gastrointest Endosc 2010;2:344. https://doi.org/10.4253/wjge.v2.i10.344.

[20] Oelfke U. Magnetic resonance imaging-guided radiation therapy: technological innovation provides a new vision of radiation oncology practice. Clin Oncol 2015;27:495–7. https://doi.org/10.1016/j.clon.2015.04.004.

[21] Van Der Horst A, Wognum S, Dávila Fajardo R, De Jong R, Van Hooft JE, Fockens P, et al. Interfractional position variation of pancreatic tumors quantified using intratumoral fiducial markers and daily cone beam computed tomography. Int J Radiat Oncol Biol Phys 2013;87:202–8. https://doi.org/10.1016/j.ijrobp.2013.05.001.

[22] Jin P, van der Horst A, de Jong R, van Hooft JE, Kamphuis M, van Wieringen N, et al. Marker-based quantification of interfractional tumor position variation and the use of markers for setup verification in radiation therapy for esophageal cancer. Radiother Oncol 2015;117:412–8. https://doi.org/10.1016/j.radonc.2015.10.005.

[23] Beltran C, Herman MG, Davis BJ. Planning target margin calculations for prostate radiotherapy based on intrafraction and interfraction motion using four localization methods. Int J Radiat Oncol Biol Phys 2008;70:289–95. https://doi.org/10.1016/j.ijrobp.2007.08.040.

[24] Gurney-Champion OJ, Lens E, Van Der Horst A, Houweling AC, Klaassen R, Van Hooft JE, et al. Visibility and artifacts of gold fiducial markers used for image guided radiation therapy of pancreatic cancer on MRI. Med Phys 2015;42:2638–47. https://doi.org/10.1118/1.4918753.

[25] Schieda N, Avruch L, Shabana WM, Malone SC. Multi-echo gradient recalled echo imaging of the pelvis for improved depiction of brachytherapy seeds and fiducial markers facilitating radiotherapy planning and treatment of prostatic carcinoma. J Magn Reson Imaging 2015;41:715–20. https://doi.org/10.1002/jmri.24590.

[26] Chan MF, Cohen GN, Deasy JO. Qualitative evaluation of fiducial markers for radiotherapy imaging. Technol Cancer Res Treat 2015;14:298–304. https://doi.org/10.1177/1533034614547447.

[27] Vorwerk H, Liersch T, Rothe H, Ghadimi M, Christiansen H, Hess CF, et al. Gold markers for tumor localization and target volume delineation in radiotherapy for rectal cancer. Strahlentherapie Und Onkol 2009;185:127–33. https://doi.org/10.1007/s00066-009-1928-5.

[28] Moningi S, Walker AJ, Malayeri AA, Rosati LM, Gearhart SL, Efron JE, et al. Analysis of fiducials implanted during EUS for patients with localized rectal cancer receiving high-dose rate endorectal brachytherapy. Gastrointest Endosc 2015;81:765–9. https://doi.org/10.1016/j.gie.2014.11.013.

[29] Dutch Trial Registry; registration no. NTR4606. Accessed July 12, 2018. n.d. http://www.trialregister.nl/trialreg/admin/rctview.asp?TC=4606.

[30] Klein S, Staring M, Murphy K, Viergever MA, Pluim JPW. Elastix: a toolbox for intensity-based medical image registration. IEEE Trans Med Imaging 2010;29:196–205. https://doi.org/10.1109/TMI.2009.2035616.

[31] Gustafsson C, Korhonen J, Persson E, Gunnlaugsson A, Nyholm T, Olsson LE. Registration free automatic identification of gold fiducial markers in MRI target delineation images for prostate radiotherapy. Med Phys 2017;44:5563–74. https://doi.org/10.1002/mp.12516.

[32] Machiels M, Van Hooft J, Jin P, Van Berge Henegouwen MI, Van Laarhoven HM, Alderliesten T, et al. Endoscopy/EUS-guided fiducial marker placement in patients with esophageal cancer: a comparative analysis of 3 types of markers. Gastrointest Endosc 2015;82:641–9. https://doi.org/10.1016/j.gie.2015.03.1972.

[33] Rydhog JS, Mortensen SR, Larsen KR, Clementsen P, Jolck RI, Josipovic M, et al. Liquid fiducial marker performance during radiotherapy of locally advanced non small cell lung cancer. Radiother Oncol 2016;121:64–9. https://doi.org/10.1016/j.radonc.2016.06.012.

[34] Schneider S, Jølck RI, Troost EGC, Hoffmann AL. Quantification of MRI visibility and artifacts at 3T of liquid fiducial marker in a pancreas tissue-mimicking phantom. Med Phys 2018;45:37–47. https://doi.org/10.1002/mp.12670.